Silencing of long non-coding RNA SDCBP2-AS1/microRNA-656-3p/CRIM1 axis promotes ferroptosis of lung cancer cells

Ninghuang Dai[1,2,3], Haitao Ma[1,4,*], Yu Feng[1]

[1] Department of Thoracic Surgery, The First Affiliated Hospital of Soochow University, Suzhou 215006, China

[2] Department of Thoracic Surgery, Nanjing Drum Tower Hospital Group Suqian Hospital, Jiangsu, Suqian 223800, China

[3] Department of Thoracic Surgery, Suqian Hospital Affiliated to Xuzhou Medical University, Jiangsu, Suqian 223800, China

[4] Department of Thoracic Surgery, Dushu Lake Hospital Affiliated to Soochow University, Suzhou 215002, China

ARTICLE INFO

ABSTRACT

Long non-coding RNAs (lncRNAs) play central roles in lung cancer progression by acting as competing endogenous RNAs (ceRNAs). This study aimed to explore the roles of lncRNA SDCBP2-AS1 in lung cancer and the molecular mechanism. The expression of SDCBP2-AS1, microRNA (miR)-656-3p, and cysteine-rich transmembrane BMP regulator 1 (CRIM1) was measured using quantitative real-time polymerase chain reaction. Ferroptosis was evaluated by analyzing cell death, ferrous content, reactive oxygen species (ROS) level, and protein levels of ferroptosis markers. The binding relationship was assessed using a dual-luciferase reporter assay. We observed that SDCBP2-AS1 was highly expressed in lung cancer cells. Knockdown of SDCBP2-AS1 promoted ferroptosis of lung cancer cells. SDCBP2-AS1 is a sponge of miR-656-3p, which directly targets CRIM1. Rescue experiments confirmed that SDCBP2-AS1 regulates ferroptosis by miR-656-3p, and overexpression of CRIM1 abrogated the effects of miR-656-3p on ferroptosis. In conclusion, depletion of SDCBP2-AS1 promoted lung cancer cell ferroptosis via the miR-656-3p/CRIM1 axis.

Introduction

Despite significant advancements in medical diagnosis and treatment, lung cancer remains the leading cause of cancer-related deaths worldwide (1). Non-small cell lung cancer (NSCLC) accounts for more than 85% of all lung cancer cases, and it is particularly prevalent in China, where it is associated with high incidence and fatality rates (2). Each year, approximately 1.8 million people are diagnosed with lung cancer globally (3). Unfortunately, many patients are diagnosed at advanced stages, limiting treatment options and increasing the risk of complications (4). While targeted therapies have improved the prognosis for some lung cancer patients, a substantial number of individuals are not suitable candidates for precision-targeted treatments. Therefore, the identification of novel therapeutic targets is urgently needed.

Long non-coding RNAs (lncRNAs) have emerged as potential targets for targeted therapy in various human diseases, including cancer (5). LncRNAs play a crucial role in the pathophysiology of lung cancer, as aberrant expression profiles of these molecules have been implicated in the disease (6). The human genome harbors numerous lncRNAs, many of which exhibit dysregulated expression during tumorigenesis and cancer progression (7). These lncRNAs regulate diverse biological functions, such as cell survival, growth, metastasis, differentiation, and cell death. Among the differentially expressed lncRNAs in lung cancer, the microarray analysis of GSE137445 has highlighted the potential high expression of the lncRNA

SDCBP2-AS1 (8). However, the precise role of SDCBP2-AS1 in lung cancer remains unclear.

Ferroptosis is a recently identified form of regulated cell death that has been associated with the progression of malignancies. It is characterized by iron-dependent lipid peroxidation, distinguishing it from other cell death modalities (9,10). Various lncRNAs have been implicated in the regulation of ferroptosis in cancer cells (11). However, studies investigating the involvement of SDCBP2-AS1 in the process of ferroptosis are currently lacking.

In the present study, we aimed to elucidate the role of SDCBP2-AS1 in lung cancer. Specifically, we sought to investigate whether SDCBP2-AS1 influences ferroptosis and to unravel the underlying molecular mechanisms involving SDCBP2-AS1 as a competing endogenous RNA (ceRNA). Through our research, we aimed to shed light on the potential of SDCBP2-AS1 as a novel therapeutic target for lung cancer.

By exploring the functional significance of SDCBP2-AS1 in lung cancer, we hope to contribute to a deeper understanding of the disease's molecular mechanisms and identify new avenues for therapeutic intervention. If SDCBP2-AS1 is found to play a substantial role in promoting lung cancer progression or inhibiting ferroptosis, it could represent a promising target for the development of innovative treatment strategies. Ultimately, our findings may lead to improved therapeutic outcomes and better prognoses for lung cancer patients.

In summary, this study aims to investigate the involvement of SDCBP2-AS1 in lung cancer and its poten-

tial impact on ferroptosis. By unraveling the molecular mechanisms underlying its role as a ceRNA, we aim to provide valuable insights into the therapeutic potential of targeting SDCBP2-AS1 in lung cancer. The identification of SDCBP2-AS1 as a novel therapeutic target could have significant implications for the management and treatment of lung cancer, addressing the critical need for alternative approaches for patients who are not suitable candidates for current targeted therapies.

Materials and Methods

Cell culture and transfection

Lung bronchial epithelial cells (Beas-2B) and lung cancer cell lines including A549, SK-MES-1, NCI-H460, and NCI-H187 were purchased from the cell bank of the Chinese Academy of Science (Shanghai, China). All cells were cultured at DMEM supplemented with 10% fetal bovine serum (FBS; Hyclone, South Logan, UT, USA) and 1% penicillin/streptomycin (Hyclone, South Logan, UT, USA) at 37°C with 5% CO_2.

Short interference RNA (siRNA)-SDCBP2-AS1 1#, siRNA-SDCBP2-AS1 2#, siRNA-negative control (NC), CRIM1 overexpression vectors, and empty vectors were obtained from Genepharma (Shanghai, China). MiR-656-3p mimic, inhibitor, miR-NC mimic, and miR-NC inhibitor were purchased from Ribobio (Guangzhou, China). The A549 cells were transfected with vectors mentioned above using the Lipofectamine 2000 reagent (Invitrogen, Carlsbad, CA, USA) for 48 h.

Propidium iodide (PI) staining assay

A549 cells were digested using 0.25% trypsin and washed using the PBS buffer. Cell concentration was adjusted to $1×10^6$ cells/mL. Then, the cells were incubated with cold 70% ethanol at 4°C overnight. After centrifugation, the cells were resuspended using normal saline. The cells (200 μL) were incubated with 2 μM Calcein-AM and 4 μM PI solution (Sigma-Aldrich, St. Louis, MO, USA) at 4°C for 30 min. The stained cells were visualized under a laser-scanning confocal microscope.

Measurement of Fe^{2+} content

A cell ferrous iron colorimetric assay kit (Elabscience, Wuhan, China) was used to measure the Fe^{2+} concentration. A549 cells ($1×10^4$) were lysed with 0.2 mL buffer solution on ice for 10 min. Following centrifugation at 15000 g for 10 min, the supernatant was collected and incubated with 80 μL chromogenic solution at 37°C for 10 min. The optical density value was measured using a microplate reader.

Determination of lipid reactive oxygen species (ROS)

C11-BODIPY 581/591 lipid peroxidation fluorescent probe (ABclonal, Wuhan, China) was used to examine the lipid ROS levels. Briefly, A549 cells were incubated with C11-BODIPY 581/591 at the final concentration of 10 μM for 1 h. After washing twice with PBS, lipid peroxidation cells were visualized with a laser-scanning confocal microscope.

Western blot

A549 cells were lysed using the radioimmunoprecipitation assay (RIPA) lysis buffer. The protein concentra-

tion was measured using the bicinchoninic acid (BCA) kit (Sangon Biotech, Shanghai, China). After the proteins were run using the 10% sodium dodecyl sulphate-polyacrylamide gel electrophoresis (SDS-PAGE), they were transferred to polyvinylidene fluoride (PVDF) membranes (Millipore, Billerica, MA, USA). The membranes were blocked using the 5% skim milk for 1 h, cultured with primary antibodies (anti-SLC7A11, anti-GPX4, anti-β-actin, Abcam, Cambridge, MA, USA) at 4°C overnight and secondary antibodies (HRP-conjugated goat anti-rabbit IgG, Abcam, Cambridge, MA, USA) at room temperature for 2 h. Finally, the protein bands were visualized using the ECL reagent (Sangon Biotech, Shanghai, China). Grey analysis was performed using the Image J software.

Bioinformatic analysis

The targets of SDCBP2-AS1 were predicted using the StarBase database. The targets of miR-636-5p were predicted using the TargetScan, miRDB, miRWalk, and starBase databases.

Dual-luciferase reporter assay

A549 cells were co-transfected with SDCBP2-AS1 wild-type (WT)/mutant plasmids and miR-636-5p/miR-NC mimic using the lipofectamine 2000 for 48 h. In addition, A549 cells were also co-transfected with CRIM1 WT/mutant plasmids and miR-636-5p/miR-NC mimic using the lipofectamine 2000 for 48 h. The luciferase activity was examined using the dual-luciferase reporter assay system (Promega, Madison, WI, USA).

Quantitative real-time polymerase chain reaction (qPCR)

Total RNA was isolated from cells using the TRIzol reagent (Invitrogen, Carlsbad, CA, USA). Following the RNA concentration was detected, 1 μg RNA was reverse transcribed to complementary deoxyribose nucleic acid (cDNA) using the cDNA reverse transcription kits (Thermo Fisher Scientific, Waltham, MA, USA). The expression of mRNA and miRNA was examined using the SYBR Green qPCR master mix (Promega, Madison, WI, USA) on ABI 7500 real-time PCR system and calculated using the $2^{-\Delta\Delta Ct}$ method. Glyceraldehyde 3-phosphate dehydrogenase (GAPDH) was the normalization for SDCBP2-AS1 and CRIM1, and U6 was the normalization for miR-656-3p.
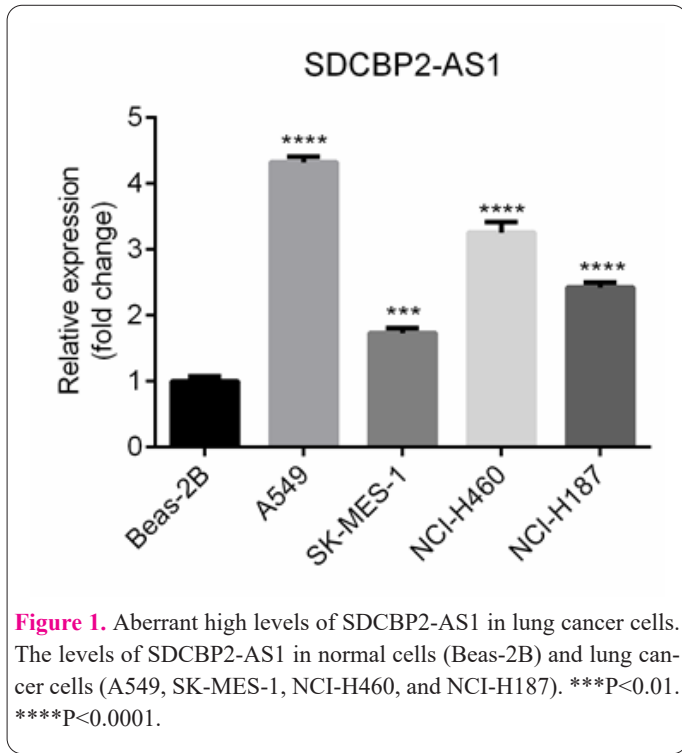
Statistical analysis

All data were analyzed using the GraphPad Prism 7.0 software (La Jolla, CA, USA). The results from three independent experiments were expressed as the mean ± standard deviation. The difference between the two groups was assessed using the student's t-test, and the difference among multiple groups was assessed using the one-way analysis of variance. $P < 0.05$ means a statistically significant difference.

Results

Aberrant high levels of SDCBP2-AS1 in lung cancer cells

The lung cancer cell lines were cultured and the expression of SDCBP2-AS1 was examined using qPCR. The results showed that SDCBP2-AS1 was significantly in-

Figure 1. Aberrant high levels of SDCBP2-AS1 in lung cancer cells. The levels of SDCBP2-AS1 in normal cells (Beas-2B) and lung cancer cells (A549, SK-MES-1, NCI-H460, and NCI-H187). ***P<0.01. ****P<0.0001.

creased in lung cancer cells, including A549, SK-MES-1, NCI-H460, and NCI-H187 cells, compared with normal Beas-2B cells (Figure 1). The SDCBP2-AS1 most upregulated A549 cells were used in the subsequent experiments.

Effects of SDCBP2-AS1 knockdown on ferroptosis of lung cancer

To identify the effects of SDCBP2-AS1 on ferroptosis, siRNA-SDCBP2-AS1 1# and siRNA-SDCBP2-AS1 2# were transfected. Compared with siRNA-NC, the levels of SDCBP2-AS1 were downregulated, especially transfection with siRNA-SDCBP2-AS1 2# (Figure 2A). Thus, siRNA-SDCBP2-AS1 2# transfected cells were used to reveal the role of SDCBP2-AS1. Cell death was analyzed using PI staining assay, and the results showed that depletion of SDCBP2-AS1 promoted cell death (Figure 2B). Fe^{2+} content was increased by the knockdown of SDCBP2-AS1 (Figure 2C). Additionally, the silencing of SDCBP2-AS1 facilitated lipid ROS production (Figure 2D). The protein levels of SLC7A11 and GPX4 were decreased by SDCBP2-AS1 loss, compared with siRNA-NC (Figure 2E).
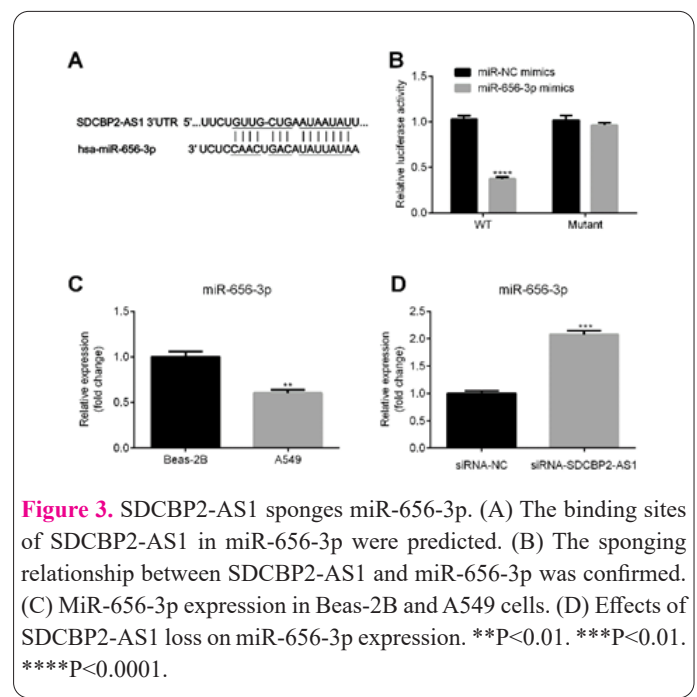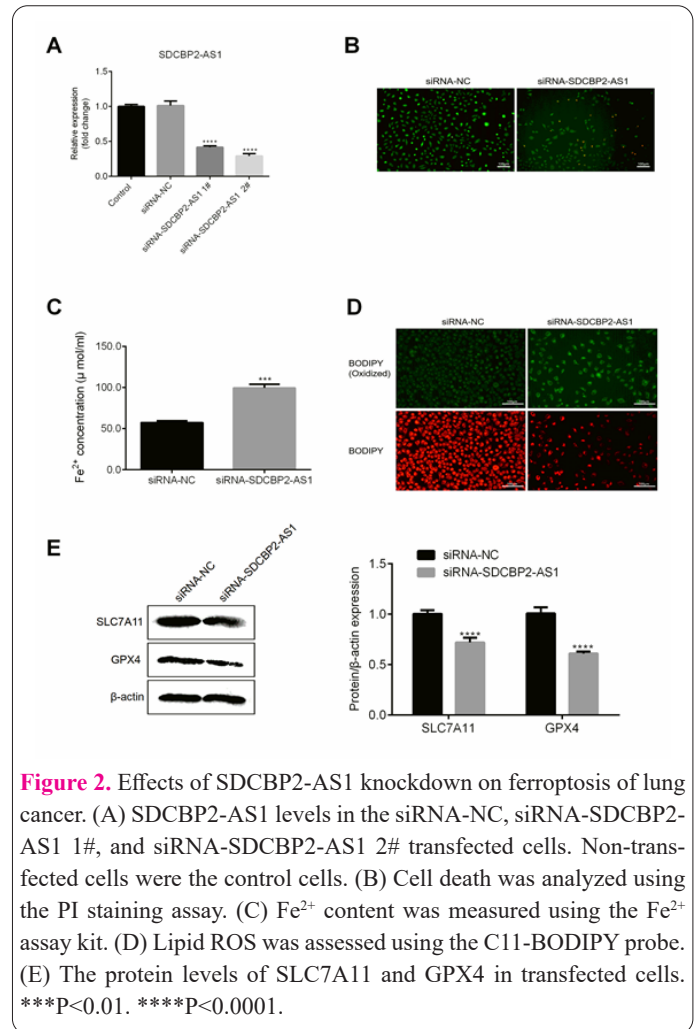
SDCBP2-AS1 sponges miR-656-3p

To explore the underlying mechanism, we predicted that SDCBP2-AS1 was a sponge of miR-656-3p (Figure 3A). Compared with miR-NC mimic, miR-656-3p reduced the luciferase activity in the SDCBP2-AS1 WT group (Figure 3B). The levels of miR-656-3p were decreased in the A549 cells, compared with the Beas-2B cells (Figure 3C). Moreover, the silencing of SDCBP2-AS1 elevated the expression of miR-656-3p in A549 cells (Figure 3D).

Downregulation of miR-656-3p reversed the ferroptosis induced by SDCBP2-AS1 knockdown

Following transfection with miR-656-3p inhibitor, the levels of miR-656-3p were reduced (Figure 4A). Cell death was promoted by the knockdown of SDCBP2-AS1, which was abolished by miR-656-3p downregulation (Fi-

gure 4B). Knockdown of SDCBP2-AS1 increased the Fe^{2+} concentration, and miR-656-3p inhibitor decreased the Fe^{2+} concentration (Figure 4C). Downregulation of miR-656-3p counteracted the increase of lipid ROS induced by SDCBP2-AS1 depletion (Figure 4D). Additionally, SDCBP2-AS1 knockdown reduced the levels of SLC7A11 and GPX4, which were rescued by the miR-656-3p inhibitor (Figure 4E).

Figure 2. Effects of SDCBP2-AS1 knockdown on ferroptosis of lung cancer. (A) SDCBP2-AS1 levels in the siRNA-NC, siRNA-SDCBP2-AS1 1#, and siRNA-SDCBP2-AS1 2# transfected cells. Non-transfected cells were the control cells. (B) Cell death was analyzed using the PI staining assay. (C) Fe^{2+} content was measured using the Fe^{2+} assay kit. (D) Lipid ROS was assessed using the C11-BODIPY probe. (E) The protein levels of SLC7A11 and GPX4 in transfected cells. ***P<0.01. ****P<0.0001.

Figure 3. SDCBP2-AS1 sponges miR-656-3p. (A) The binding sites of SDCBP2-AS1 in miR-656-3p were predicted. (B) The sponging relationship between SDCBP2-AS1 and miR-656-3p was confirmed. (C) MiR-656-3p expression in Beas-2B and A549 cells. (D) Effects of SDCBP2-AS1 loss on miR-656-3p expression. **P<0.01. ***P<0.01. ****P<0.0001.

Figure 4. Downregulation of miR-656-3p reversed the ferroptosis induced by SDCBP2-AS1 knockdown. (A) miR-656-3p levels in the miR-NC inhibitor and miR-656-3p inhibitor transfected cells. (B) Cell death was analyzed using the PI staining assay. (C) Fe^{2+} concentration was measured using the Fe^{2+} assay kit. (D) Lipid ROS was assessed using the C11-BODIPY probe. (E) The protein levels of SLC7A11 and GPX4 in transfected cells. *P<0.05. ***P<0.01. ****P<0.0001.

miR-656-3p targets CRIM1

To explore the molecular mechanism of miR-656-3p, we used bioinformatic analysis to predict the targets of miR-656-3p. A total of 69 targets were identified from the TargetScan, miRDB, miRWalk, and starBase online databases (Figure 5A). Among them, CRIM1 has the binding sites of miR-656-3p (Figure 5B). Overexpression of miR-656-3p reduced the luciferase activity in the CRIM1 WT group, compared with miR-NC mimic (Figure 5C). The expression of CRIM1 was higher in the A549 cells than that in the Beas-2B cells (Figure 5D). Downregulation of miR-656-3p elevated CRIM1 levels and knockdown of SDCBP2-AS1 rescued the elevation of CRIM1 induced by miR-656-3p downregulation (Figure 5E).

CRIM1 abrogated the ferroptosis induced by miR-656-3p

Following transfection with miR-656-3p mimic, the expression of miR-656-3p was increased (Figure 6A). In addition, CRIM1 was upregulated after transfection with CRIM1 overexpression vectors (Figure 6B). Cell death induced by miR-656-3p was abrogated by CRIM1 overexpression (Figure 6C). Overexpression of miR-656-3p increased the Fe^{2+} concentration, whereas CRIM1 reversed the increase (Figure 6D). Lipid ROS was increased by miR-656-3p, and CRIM1 counteracted the increase induced by miR-656-3p (Figure 6E). The expression of SLC7A11 and GPX4 at protein levels was decreased by miR-656-3p, while CRIM1 rescued the decrease (Figure 6F).

Discussion

Lung cancer is a very high incidence of cancer with a poor prognosis. LncRNAs are identified to be biomarkers for cancer diagnosis, prognosis, and targets for cancer therapy (12). Previous studies have revealed that several lncRNAs participate in lung cancer progression by mediating ferroptosis. For instance, curcumenol inhibits cell viability and triggers ferroptosis of lung cancer cells, and loss of lncRNA H19 promoted ferroptosis induced by curcumenol (13). LINC00336 interacts with MIR6852 to suppress ferroptosis by sponging ELAVL1 in lung cancer cells (14). Additionally, lncRNA MT1DP exacerbates oxidative stress and sensitives to ferroptosis in A549 and H1299 cells by mediating the miR-365a-3p/NRF2 axis (15). SDCBP2-AS1 is downregulated in ovarian cancer, and overexpression of which inhibits cell viability, migration, and invasion (16). Moreover, SDCBP2-AS1 levels were decreased in patients with osteoporosis (17). Downregulation of SDCBP2-AS1 is linked to the longer survival rate of patients with thyroid cancer (18). In the present study, we investigated the role of SDCBP2-AS1 in lung cancer, which has not been reported previously. SDCBP2-AS1 was upregulated in lung cancer cells. Knockdown of SDCBP2-AS1 inhibited cell death, increased Fe^{2+} concentration and lipid ROS levels, and downregulated SLC7A11 and GPX4 levels, suggesting that SDCBP2-AS1 depletion promoted ferroptosis in lung cancer cells. SDCBP2-AS1 functioned as an oncogene in lung cancer.

LncRNAs participate in competitive regulation, acting as sponges for miRNAs to regulate gene expression
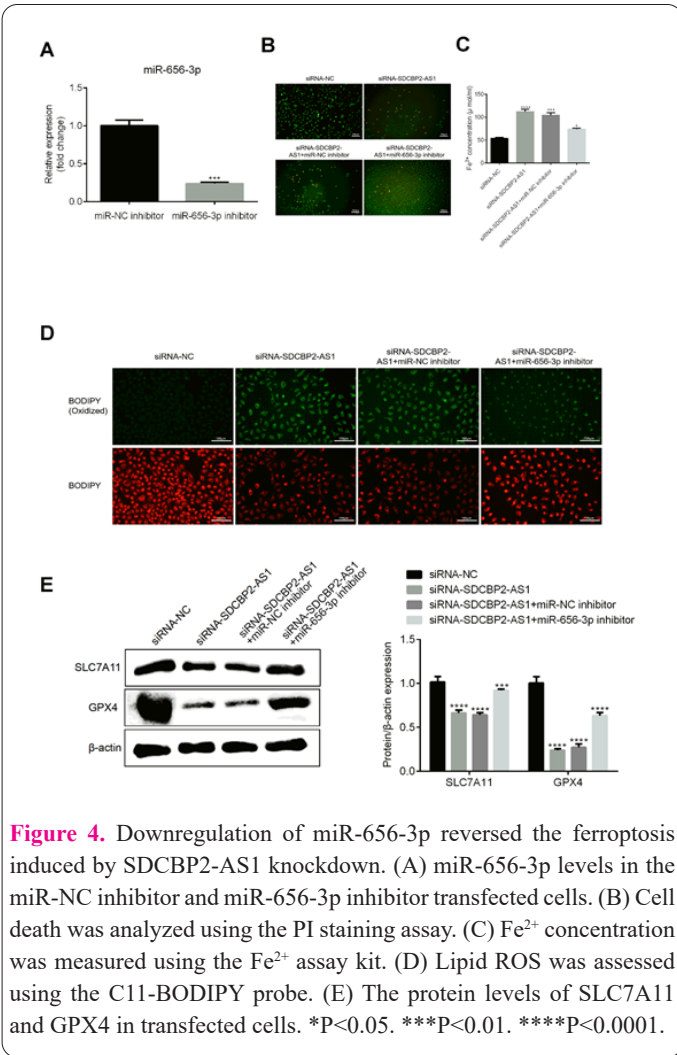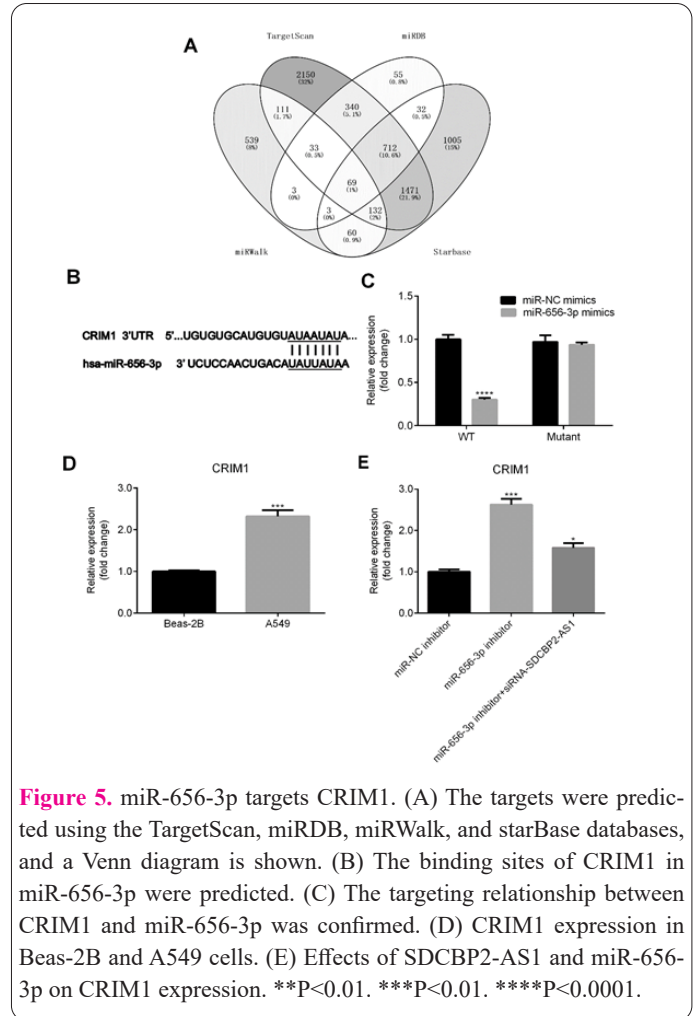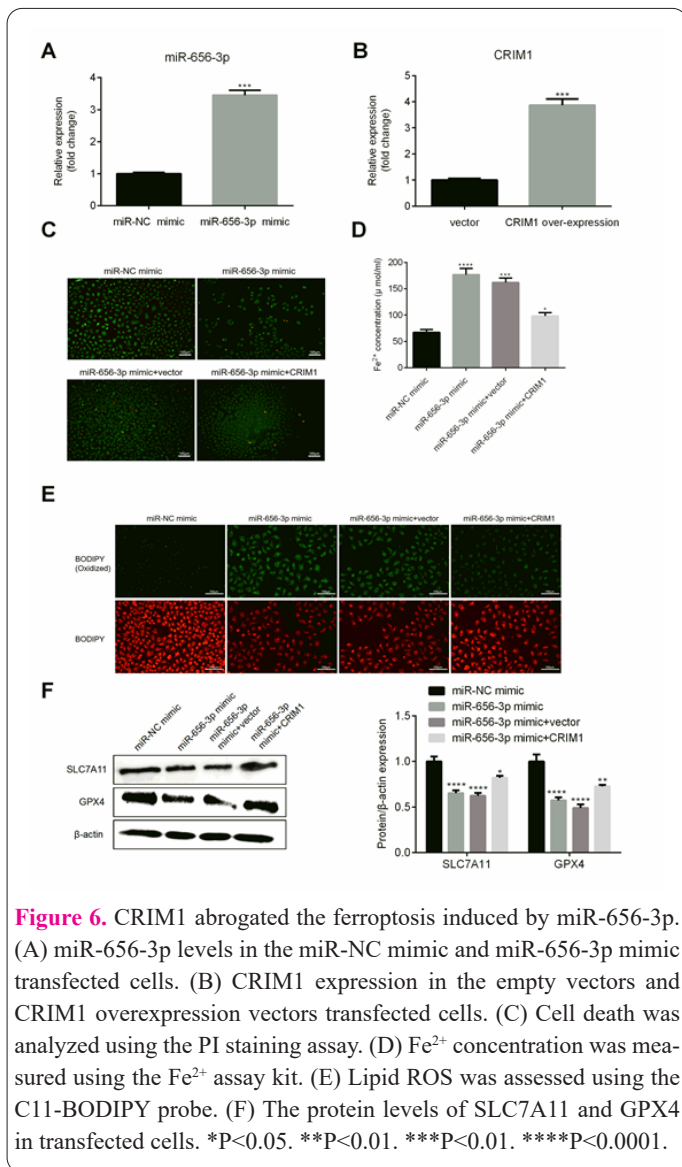

Figure 5. miR-656-3p targets CRIM1. (A) The targets were predicted using the TargetScan, miRDB, miRWalk, and starBase databases, and a Venn diagram is shown. (B) The binding sites of CRIM1 in miR-656-3p were predicted. (C) The targeting relationship between CRIM1 and miR-656-3p was confirmed. (D) CRIM1 expression in Beas-2B and A549 cells. (E) Effects of SDCBP2-AS1 and miR-656-3p on CRIM1 expression. **P<0.01. ***P<0.01. ****P<0.0001.

Figure 6. CRIM1 abrogated the ferroptosis induced by miR-656-3p. (A) miR-656-3p levels in the miR-NC mimic and miR-656-3p mimic transfected cells. (B) CRIM1 expression in the empty vectors and CRIM1 overexpression vectors transfected cells. (C) Cell death was analyzed using the PI staining assay. (D) Fe^{2+} concentration was measured using the Fe^{2+} assay kit. (E) Lipid ROS was assessed using the C11-BODIPY probe. (F) The protein levels of SLC7A11 and GPX4 in transfected cells. *P<0.05. **P<0.01. ***P<0.01. ****P<0.0001.

(19). MiR-656-3p is a tumor suppressor in cancers, such as nasopharyngeal carcinoma (20), liver cancer (21), and colorectal cancer (22). In NSCLC, downregulation of miR-656-3p counteracted the suppression of cell proliferation, glycolysis, invasion, and migration induced by circular RNA 0018189 deficiency (23). Additionally, miR-656-3p impairs NSCLC cell proliferation and migration (24). In this study, we confirmed that SDCBP2-AS1 is a sponge of miR-656-3p. We first identified that downregulation of miR-656-3p abrogated the effects on ferroptosis induced by SDCBP2-AS1 loss, suggesting that silencing of SDCBP2-AS1 facilitated ferroptosis by absorbing miR-656-3p.

CRIM1 is a bone morphogenetic protein antagonist member. CRIM1 is involved in the regulation of embryonic development, angiogenesis, organogenesis, and disease pathology (25). It is newly identified to promote tumor cell migration and adhesion in lung cancer (26). In addition, CRIM1 may be a prognosis biomarker of lung cancer (27). However, whether CRIM1 was associated with ferroptosis remains unknown. Herein, we clarified that miR-656-3p directly targets CRIM1. Overexpression of CRIM1 rescued the effects of miR-656-3p on ferroptosis in lung cancer cells. The data suggested that miR-656-3p promoted ferroptosis by targeting CRIM1.

The present comprehensive investigation presented in the manuscript titled "Silencing of long non-coding RNA SDCBP2-AS1/microRNA-656-3p/CRIM1 axis promotes ferroptosis of lung cancer cells" provides valuable insights into the potential therapeutic implications of targeting SDCBP2-AS1 in lung cancer. The study demonstrated that SDCBP2-AS1 is significantly upregulated in lung cancer, suggesting its potential role as a biomarker for the disease. By employing a silencing strategy, the researchers successfully disrupted the expression of SDCBP2-AS1 in A549 cells, leading to the induction of ferroptosis, an iron-dependent form of regulated cell death. This finding highlights the crucial involvement of SDCBP2-AS1 in regulating cellular processes and survival mechanisms in lung cancer cells. Further investigation revealed that SDCBP2-AS1 functions as a competing endogenous RNA (ceRNA) by sequestering miR-656-3p, a microRNA with known roles in cancer development and progression. By acting as a sponge for miR-656-3p, SDCBP2-AS1 effectively modulates the expression of its downstream target, CRIM1, which is implicated in various cellular pathways, including those associated with cancer. The observed regulation of ferroptosis through the SDCBP2-AS1/miR-656-3p/CRIM1 axis provides a mechanistic understanding of how SDCBP2-AS1 influences lung cancer cell survival. Targeting SDCBP2-AS1, either directly or by manipulating the miR-656-3p/CRIM1 axis, holds promise as a potential therapeutic strategy for lung cancer. By disrupting the delicate balance of this regulatory network, it may be possible to induce ferroptosis and promote tumor cell death.

Conclusion

These findings shed light on the complex molecular mechanisms underlying lung cancer progression and provide a foundation for future investigations into novel therapeutic approaches. Further studies are warranted to explore the clinical relevance of SDCBP2-AS1 as a diagnostic biomarker and its potential as a therapeutic target for lung cancer patients. Ultimately, these efforts may contribute to the development of more effective treatment strategies and improved patient outcomes in the battle against lung cancer.

Funding
The authors declare that no funds, grants, or other support were received during the preparation of this manuscript.

Competing Interests
The authors have no relevant financial or non-financial interests to disclose.

Author Contributions
All authors contributed to the study's conception and design. Material preparation, data collection and analysis were performed by Ninghuang Dai and Yu Feng. The first draft of the manuscript was written by Ninghuang Dai and all authors commented on previous versions of the manuscript. All authors read and approved the final manuscript.

Ethics approval
No ethical approval is required.

Data available
All data generated or analyzed during this study are in-

cluded in this article. Further enquiries can be directed to the corresponding author.

References

1. Bade BC, Dela CC. Lung Cancer 2020: Epidemiology, Etiology, and Prevention. Clin Chest Med 2020; 41(1): 1-24.

2. Wu F, Wang L, Zhou C. Lung cancer in China: current and prospect. Curr Opin Oncol 2021; 33(1): 40-46.

3. Ma J, Yu D, Zhao D, et al. Poly-Lactide-Co-Glycolide-Polyethylene Glycol- Ginsenoside Rg3-Ag Exerts a Radio-Sensitization Effect in Non-Small Cell Lung Cancer. J Biomed Nanotechnol 2022; 18(8): 2001-2009.

4. Zhang Y, Gu M. Experimental Study on Antitumor Activity of Gold Nanoparticles-Assisted Delivery of PD-L1 SiRNA in Non-Small Cell Lung Cancer. J Biomed Nanotechnol 2022; 18(5): 1521-1526.

5. Winkle M, El-Daly SM, Fabbri M, Calin GA. Noncoding RNA therapeutics - challenges and potential solutions. Nat Rev Drug Discov 2021; 20(8): 629-651.

6. Chen R, Li WX, Sun Y, et al. Comprehensive Analysis of lncRNA and mRNA Expression Profiles in Lung Cancer. Clin Lab 2017; 63(2): 313-320.

7. Zhou B, Yang H, Yang C, et al. Translation of noncoding RNAs and cancer. Cancer Lett 2021; 497: 89-99.

8. Song H, Li H, Ding X, et al. Long non-coding RNA FEZF1-AS1 facilitates non-small cell lung cancer progression via the ITGA11/miR-516b-5p axis. Int J Oncol 2020; 57(6): 1333-1347.

9. Mou Y, Wang J, Wu J, et al. Ferroptosis, a new form of cell death: opportunities and challenges in cancer. J Hematol Oncol 2019; 12(1): 34.

10. Wu S, Zhu C, Tang D, Dou QP, Shen J, Chen X. The role of ferroptosis in lung cancer. Biomark Res 2021; 9(1): 82.

11. Tang R, Wu Z, Rong Z, et al. Ferroptosis-related lncRNA pairs to predict the clinical outcome and molecular characteristics of pancreatic ductal adenocarcinoma. Brief Bioinform 2022; 23(1): bbab388.

12. 12. Zhang S, Zhu K, Han Q, Wang Q, Yang B. lncRNA PCAT1 might coordinate ZNF217 to promote CRC adhesion and invasion through regulating MTA2/MTA3/Snai1/E-cadherin signaling. Cell Mol Biol 2021; 67(4): 1-9.

13. Zhang R, Pan T, Xiang Y, et al. Curcumenol triggered ferroptosis in lung cancer cells via lncRNA H19/miR-19b-3p/FTH1 axis. Bioact Mater 2022; 13: 23-36.

14. Wang M, Mao C, Ouyang L, et al. Long noncoding RNA LINC00336 inhibits ferroptosis in lung cancer by functioning as a competing endogenous RNA. Cell Death Differ 2019; 26(11): 2329-2343.

15. Gai C, Liu C, Wu X, et al. MT1DP loaded by folate-modified liposomes sensitizes erastin-induced ferroptosis via regulating miR-365a-3p/NRF2 axis in non-small cell lung cancer cells. Cell Death Dis 2020; 11(9): 751.

16. Liu X, Liu C, Zhang A, et al. Long non-coding RNA SDCBP2-AS1 delays the progression of ovarian cancer via microRNA-100-5p-targeted EPDR1. World J Surg Oncol 2021; 19(1): 199.

17. Centofanti F, Santoro M, Marini M, et al. Identification of Aberrantly-Expressed Long Non-Coding RNAs in Osteoblastic Cells from Osteoporotic Patients. Biomedicines 2020; 8(3): 65.

18. Rao Y, Liu H, Yan X, Wang J. In Silico Analysis Identifies Differently Expressed lncRNAs as Novel Biomarkers for the Prognosis of Thyroid Cancer. Comput Math Method M 2020; 2020: 3651051.

19. Kanabe BO, Ozaslan M, Aziz SA, Al-Attar MS, Kilic IH, Khailany RA. Expression patterns of LncRNA-GAS5 and its target APOBEC3C gene through miR-103 in breast cancer patients. Cell Mol Biol 2021; 67(3): 5-10.

20. Tian X, Liu Y, Wang Z, Wu S. lncRNA SNHG8 promotes aggressive behaviors of nasopharyngeal carcinoma via regulating miR-656-3p/SATB1 axis. Biomed Pharmacother 2020; 131: 110564.

21. Li G, Du P, He J, Li Y. CircRNA circBACH1 (hsa_circ_0061395) serves as a miR-656-3p sponge to facilitate hepatocellular carcinoma progression through increasing SERBP1 expression. Biochem Bioph Res Co 2021; 556: 1-8.

22. Zhang B, Gao S, Bao Z, Pan C, Tian Q, Tang Q. MicroRNA-656-3p inhibits colorectal cancer cell migration, invasion, and chemo-resistance by targeting sphingosine-1-phosphate phosphatase 1. Bioengineered 2022; 13(2): 3810-3826.

23. Cai J, Zheng Y, Dong L, Zhang X, Huang Y. Circular RNA hsa_circ_0018189 drives non-small cell lung cancer growth by sequestering miR-656-3p and enhancing xCT expression. J Clin Lab Anal 2022; 36(11): e24714.

24. Chen T, Qin S, Gu Y, Pan H, Bian D. Long non-coding RNA NORAD promotes the occurrence and development of non-small cell lung cancer by adsorbing MiR-656-3p. Mol Genet Genom Med 2019; 7(8): e757.

25. Zeng H, Tang L. CRIM1, the antagonist of BMPs, is a potential risk factor of cancer. Curr Cancer Drug Tar 2014; 14(7): 652-658.

26. Zeng H, Zhang Y, Yi Q, Wu Y, Wan R, Tang L. CRIM1, a new-found cancer-related player, regulates the adhesion and migration of lung cancer cells. Growth Factors 2015; 33(5-6): 384-392.

27. Han X, Ren P, Ma S. Bioinformatics analysis reveals three key genes and four survival genes associated with youth-onset NSCLC. Open Med-Warsaw 2022; 17(1): 1123-1133.